An experimental study of effect of printed thickness on the mechanical properties of LPBF produced AlSi10Mg

FAHIMI Pouya[1,a] *, VYSOCHINSKIY Dmitry[2,b] and KHADYKO Mikhail[1,c]

[1]Department of Building, Energy and Material Technology, UiT-The Arctic University of Norway, Narvik, Norway

[2]Jon Lilletuns vei 9, 4879, Grimstad, Mechatronics Innovation Lab, Norway

[a]pouya.fahimi@uit.no, [b]dmitry.vysochinskiy@uia.no, [c]mikhail.khadyko@uit.no

Keywords: Selective Laser Melting, Size Effect, AlSi10Mg, Metal Additive Manufacturing, Tensile Testing, Powder Bed Fusion

Abstract. Additive manufacturing process allows fabrication of parts with a broad range of sizes with high resolution. This size variation introduces new mechanical properties within the printed component, which creates a significant challenge for the qualification of additively manufactured parts. This unresolved issue hinders the implementation of additive manufacturing in high performance engineering applications. To attain optimal performance of additive components, it is imperative to gain a comprehensive understanding of the size effect. While many studies have explored the mechanical properties and microstructure of additively manufactured AlSi10Mg, the size effect remains relatively undefined. To gain more knowledge on this matter, AlSi10Mg samples with four different thicknesses were fabricated using a selective laser melting machine and tensile tests were performed to characterize the material behavior. Stress-strain curves were derived with consideration of nominal and measured cross section and the resulting diagram showed a considerable difference for the samples with minimum thickness, which was 0.5 mm. Comparing the results between the 2 mm and 0.5 mm thick specimens demonstrated more than 50 percent decrease in tensile properties including ultimate tensile strength and elongation at fracture. Also, the study of strain rate indicated no significant strain rate sensitivity for either thickness. These findings contribute to better understanding the size effects on behavior of printed AlSi10Mg, promoting further commercial adoption of this material.

Introduction

Additive manufacturing (AM), also known as 3D printing, is a rapidly growing technology that allows for the creation of complex and detailed objects by building up layers of material [1-3]. It offers a wide variety of process categories to suit different needs and applications. These processes allow to produce complex geometries with unique properties that would be difficult or impossible to produce using traditional manufacturing techniques. As this technology continues to advance, it has the potential to revolutionize the manufacturing industry and create new opportunities for innovation and growth. Metal additive manufacturing is a process that involves joining metallic materials, such as powders, wires, and sheets, to produce objects from 3D models, typically layer by layer [4-7].

While various metal additive manufacturing processes share similar capabilities and challenges, the focus of the current study lies in selective laser melting (SLM) which is a type of laser powder bed fusion (LPBF). In this process, a laser beam draws onto a bed of thin layer of powder, melting the powder along the laser path to create a solid layer of the part. Subsequently, with the aid of the recoating mechanism, a new layer of powder is applied over the part, and the 3D structure is incrementally built layer by layer.

Recent research on additively manufactured metallic parts indicates that mechanical properties may depend on many factors of the printing process particularly building orientation [8-12], laser power [13], scan strategies [14, 15] and feature size [16]. One reason behind this difference in material behavior is thermal gradients inducing directional solidification and as a result there might be anisotropic microstructures and crystallographic texture. Consequently, this phenomenon can result in anisotropic mechanical behavior in the manufactured component. Also, the size of the printed part can affect the properties and performance of the final product. One reason behind this alteration of behavior is the size effect on the microstructure of the printed part. As the size of the part increases, the heat generated by the laser during printing and the cooling rate can vary across the part, leading to a non-uniform microstructure. This can result in variations in material properties such as mechanical strength and hardness. Another size effect is related to the level of residual stress in the printed part. Residual stresses are generated during the printing process due to non-uniform cooling and solidification of the material.

The considerable design flexibility offered by 3D printing allows for versatile creation of AM parts. In many cases, these parts include a diverse range of feature sizes, with users usually showing particular interest in smaller features. Therefore, understanding the size effect becomes essential for making informed and effective design decisions and accordingly there is ongoing research in the field of additive manufacturing to address this. For example, Takata et al. [17] investigated the size dependence of microstructure of AlSi10Mg plate samples ranging from 0.1 to 10 mm and observed a slight effect on microstructure with variation of thickness. They also reported a slight decrease of hardness with decreasing the sample width. Dong et al. [16] tested a series of additively manufactured rod shape samples made of AlSi10Mg. Their results of the uniaxial tensile test indicate that as the build diameter decreases, both the strength and Young's modulus of the specimen decrease by 30% compared to the stable state. Another interesting study in this field is the work done by Roach et al. [18] where they investigated the size-dependent tensile properties of 316L stainless steel. They scaled down their whole specimen shape and observed that the ultimate tensile strength decreased drastically with decreasing specimen size. They also reported that the surface roughness is the reason for this change in material behavior rather than the change in the microstructure. Moreover, Barba et al. [19] carried out a similar study for size and orientation effect in additively manufactured Ti-6Al-4V. They examined tensile specimens with varying thickness from 0.25 to 3 mm and their result showed a high dependency of material properties on the specimen thickness.

In summary, a review of prior studies indicates that the process parameters in SLM play a crucial role in influencing the microstructure's heterogeneity and the macroscopic performance of fabricated structures. However, existing research has predominantly centered on factors such as the orientation dependence and there is a scarcity of studies investigating the influence of the size effect on mechanical properties of additively manufactured aluminum tensile samples. So, the primary objective of this study is to examine the impact of size on the mechanical properties of AlSi10Mg flat tensile samples fabricated with SLM. Flat tensile samples with four different thickness dimensions were manufactured and uniaxial tensile tests were carried out on as-built samples.

Materials and Methods
Four sets of flat tensile specimens with varied thicknesses were made to investigate the mechanical responses. Detailed descriptions of the manufacturing process and experimental investigation are described as follows. AlSi10Mg powder produced in TEKNA advanced material [20] was utilized as a raw material in this study. The chemical composition of the powder is 10 %wt of Si and 0.3 %wt Mg. The specimen dimensions are depicted in Fig. 1a, all the dimensions are in millimeters. The smallest thickness is 0.5 mm which is close to the minimum thickness that is feasible to print by SLM-process and the other thicknesses are 1, 1.5 and 2 mm. It should be noted that these

dimensions are not exactly in accordance with the standards of tensile testing, however, some general considerations for preparing tensile testing samples have been taken into account based on ISO 6892-1 [21]. The specimens were manufactured using a SLM®280 [22] metal printer with an output laser power of 400W and argon gas was chosen to be the build atmosphere. A schematic of the scanning strategy is depicted in Fig. 1b. The layer thickness was set to 50 μm. Arrows in Fig. 1b displays the path of movement of the laser, and the correspondence between their color, power and scanning speed is reported in Table 1. Uniaxial tension tests were conducted using a 25 kN SI-plan tension machine equipped with hydraulic grips. The machine features a load cell, a built-in position sensor, and an attachable LVDT-based extensometer with a measurement range of 25 mm to 30 mm. Load-displacement curves were generated using the output of the tensile testing machine. Fig. 1c is a picture of the build plate (after removing the printed parts) on the machine and as it can be seen from Fig. 1d, the samples of this work are a part of bigger print and the place that the tensile specimens are cut down from is shown by a red rectangle in the picture. All the samples were printed vertically on a square shaped build plate with a size of 278 mm by 278 mm.
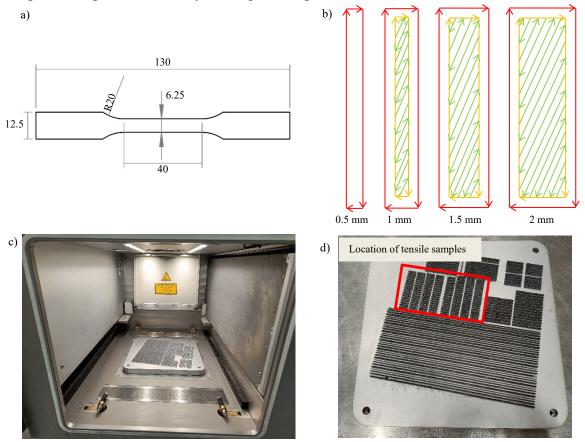

Fig. 1 a) Tensile sample geometry b) Schematic of scanning pattern for different thickness sizes in the gauge part of the samples c) Picture of the built plate inside of the working area of the machine d) Picture of the build plate after cutting down the samples.

Table 1. Processing parameters for the SLM machine

Parameter	Red border	Orange border	Green in-skin
Laser power (W)	370	350	300
Laser speed (mm/s)	860	1100	600

Results

A total number of 41 tensile tests on as-built samples were conducted to examine the mechanical response and statistical variations related to specimen thickness size. Quasi-static tensile tests until failure were carried out at a constant displacement rate of 0.025 mm.s^{-1} and room temperature approximately 20°C. Variation of yield strength, ultimate tensile strength and elongation at fracture for different thickness values are represented in Fig. 2. There were no statistically significant differences in strength properties between specimens of the same thickness. The bars in Fig. 2 are showing the average value and error bars denote one standard deviation. Number of tests with usable results for 0.5, 1-, 1.5- and 2-mm samples are respectively 10, 13, 6 and 12. A general increase of elongation at fracture can be observed from the results, where the average elongation at fracture for the specimens with 2 mm thickness is more than two times of the ones with 0.5 mm thickness. In addition, a broad range of elongation to failure was observed among all sample sizes, which is a characteristic of 3D printed manufactured parts that many researchers have observed [18]. Furthermore, the average ultimate tensile strength increases with increasing the thickness and the range of the ultimate tensile strength for 1, 1.5 and 2 mm thicknesses is consistent with the ones reported in the literature [23]. However, the samples with 0.5 mm thickness show a significantly lower ultimate tensile strength. Similar results are also observed for the yield strength.
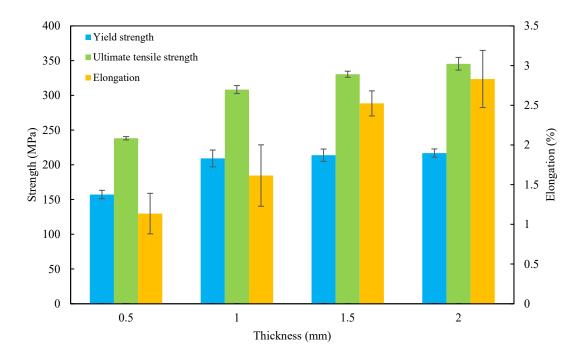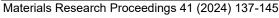

Fig. 2 Variation of average yield strength, ultimate tensile strength, and elongation at fracture for different thickness of the samples. Error bars indicate one standard deviation.

Additionally, load-displacement diagrams for different thicknesses are displayed in Fig. 3. A general consistency of the results of each thickness can be observed from the diagrams. Although, in a few cases slippage of the extensometer on the machine has occurred and caused a deviation from the general trend and for some tests this slippage has occurred very early during the experiment and caused a huge error. The results of these tests are not reported here. Samples display a semi brittle behavior, experiencing failure after undergoing some plastic deformation but before the formation of a neck. No consistently specific location of breakage in different specimens was observed.
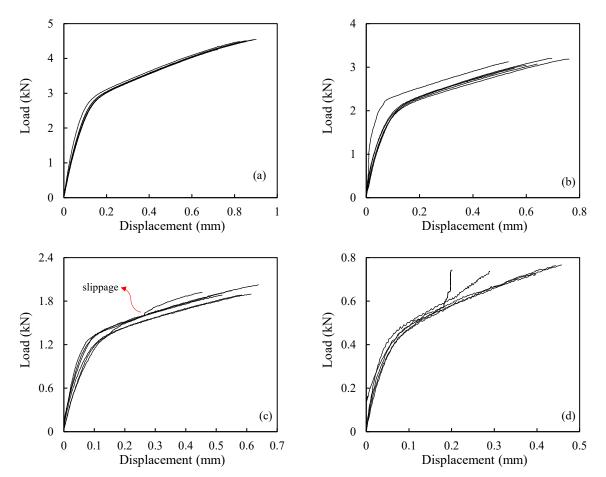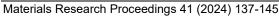
Fig. 3 Load-Displacement diagram for all samples: a) 2 mm thickness samples b) 1.5 mm thickness samples c) 1 mm thickness samples d) 0.5 mm thickness samples.

Fig. 4 demonstrates the engineering stress versus engineering strain curves for variation of thickness. Three different test results for each thickness have been displayed in these figures and each thickness is displayed with its own distinct color in the diagram. For Fig. 4a the nominal cross-section has been used and for Fig. 4b measured cross-section has been considered. Both cross-section measurements are referring to the initial section area before the tensile test. For considering the measured cross-section, the thickness and width of each sample has been measured three times at different random locations and then an average of the measured values was found. The difference between the average measured width and nominal width of the samples was less than one percent. So, it was assumed that the measured width for all of the samples is equal to the nominal width which is 6.25 mm and only the thickness measurement has defined the difference between the nominal and measured cross-section areas. It should be also noted that, for the samples with 0.5 mm thickness the average measured thickness was 0.58 mm which produces a huge difference in the stress between the nominal results and measured results. For the other samples the difference between the nominal and measured thickness is much less significant. Also, the considerable difference in the stress levels between the 0.5 mm samples and the other thicknesses becomes even larger when the measured cross-sections is used.
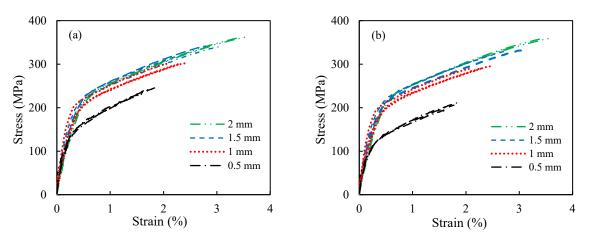
Fig. 4 Stress-Strain curve for variation of the thickness a) Nominal cross section b) Measured cross section.

To study the strain rate effect, 12 more tests have been performed for 0.5 mm and 1 mm thickness samples and the results are reported in Fig. 5 and Fig. 6. These additional tests are performed at 0.1 and 0.005 mm.s⁻¹ displacement rates with three tests for each thickness at each displacement rate. Nominal cross-section has been considered for the engineering stress-strain curves in this case. According to Fig. 5, for 1 mm thickness samples the stress is generally reduced with increased strain rate, but no such trend can be observed for the results of 0.5 mm thickness tests, where the stress is not affected by the strain rate.
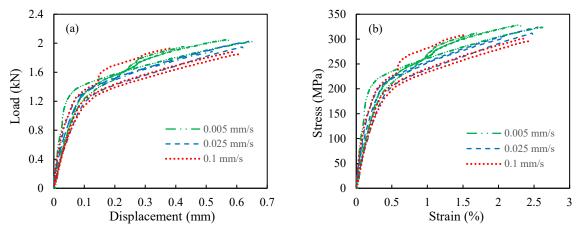

Fig. 5 Strain rate variation for the samples with 1 mm thickness a) Load-Displacement diagram b) Stress-Strain curve.
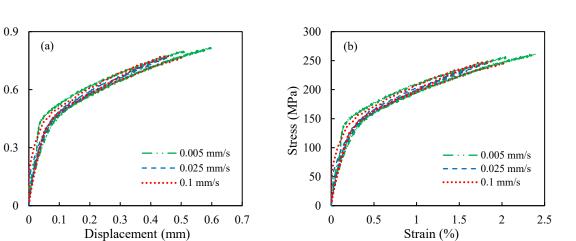
Fig. 6 Strain rate variation for the samples with 0.5 mm thickness a) Load-Displacement diagram b) Stress-Strain curve.

Summary and Discussion

Uniaxial tensile tests were performed on AlSi10Mg as-built samples with 4 different thicknesses. The results show a trend of decreasing ultimate tensile strength with decreasing sample thickness. Another trend is a consistent increase in elongation at fracture with increasing thickness, where the average elongation at fracture for the specimens with 2 mm thickness are more than twice that of the specimens with 0.5 mm thickness. Moreover, samples with a thickness of 0.5 mm exhibit significantly lower strength compared to the larger thickness samples. One likely reason for the differences can be different input energy and scanning speed. As the schematic picture displayed in Fig. 1b indicates, for the 0.5 mm thickness, the cross-section of the specimen is made by only two passes of the laser beam over the powder and the laser power and speed for the border of the cross-section is different from the in-skin of the cross-section. Therefore, the material of specimens with different thicknesses has different thermal history, resulting in different material properties. Observation of the surface of samples (even without magnification) also indicates a difference in the surface roughness and morphology between 0.5 mm thickness samples and other samples. Accordingly, as the sample size decreases, there might be microstructural alterations which are attributed to variations in the ratio between border and in-skin laser strategies. Therefore, conducting a follow-up study on the properties created by different scanning strategies would be beneficial in providing further clarity on this issue.

The work done by [24] is an experimental study similar to this work with the same material and printing machine, but a different size and shape of the samples. Comparing the presented results with the results of this study shows the same trend of a general decrease in strength with decreasing size. For the 2 mm samples in the present work the average ultimate strength is about 15% lower than for the ones reported in [24].

Stress-strain curves were calculated based on two different cross-section considerations: nominal and measured. In the case of samples with a thickness of 0.5 mm, the average measured thickness was 0.58 mm, signifying a substantial difference between the nominal and measured results. Furthermore, the significant difference in the behavior of the 0.5 mm samples, in comparison to other thicknesses, becomes even more evident when measured cross-sections are utilized. According to the results with variation of strain rate, for samples with a thickness of 1 mm, the stress-strain curve generally shifts downward with an increase in strain rate. In contrast, no noticeable trend is observed in the results for 0.5 mm thickness, indicating no significant change with varying strain rates.

The observed reduction in strength for smaller thicknesses can result in significant discrepancies between expected and actual material performance. Designers utilizing additive manufacturing components must be considerate of this and utilize corrective measures. This includes incorporating an effective feature thickness and employing an appropriate material model parameters to ensure accurate and reliable performance of components.

References

[1] X.Y. Cheng, S.J. Li, L.E. Murr, Z.B. Zhang, Y.L. Hao, R. Yang, F. Medina and R.B. Wicker, Compression deformation behavior of Ti-6Al-4V alloy with cellular structures fabricated by electron beam melting, J Mech Behav Biomed Mater. 16 (2012) 153-62. https://doi.org/10.1016/j.jmbbm.2012.10.005

[2] O. Al-Ketan, R. Rowshan and R.K. Abu Al-Rub, Topology-mechanical property relationship of 3D printed strut, skeletal, and sheet based periodic metallic cellular materials, Addit. Manuf. 19 (2018) 167-183. https://doi.org/10.1016/j.addma.2017.12.006

[3] C. Yan, L. Hao, A. Hussein and P. Young, Ti-6Al-4V triply periodic minimal surface structures for bone implants fabricated via selective laser melting, J Mech Behav Biomed Mater. 51 (2015) 61-73. https://doi.org/10.1016/j.jmbbm.2015.06.024

[4] D. Herzog, V. Seyda, E. Wycisk and C. Emmelmann, Additive manufacturing of metals, Acta Mater. 117 (2016) 371-392. https://doi.org/10.1016/j.actamat.2016.07.019

[5] W.E. Frazier, Metal Additive Manufacturing: A Review, J. Mater. Eng. Perform. 23(6) (2014) 1917-1928. https://doi.org/10.1007/s11665-014-0958-z

[6] B. Blakey-Milner, P. Gradl, G. Snedden, M. Brooks, J. Pitot, E. Lopez, M. Leary, F. Berto and A. du Plessis, Metal additive manufacturing in aerospace: A review, Mater. Des. 209 (2021). https://doi.org/10.1016/j.matdes.2021.110008

[7] S. Cooke, K. Ahmadi, S. Willerth and R. Herring, Metal additive manufacturing: Technology, metallurgy and modelling, J. Manuf. Process. 57 (2020) 978-1003. https://doi.org/10.1016/j.jmapro.2020.07.025

[8] A. Tridello, J. Fiocchi, C.A. Biffi, G. Chiandussi, M. Rossetto, A. Tuissi and D.S. Paolino, Effect of microstructure, residual stresses and building orientation on the fatigue response up to 109 cycles of an SLM AlSi10Mg alloy, Int. J. Fatigue. 137 (2020). https://doi.org/10.1016/j.ijfatigue.2020.105659

[9] C.G. Wang, J.X. Zhu, G.W. Wang, Y. Qin, M.Y. Sun, J.L. Yang, X.F. Shen and S.K. Huang, Effect of building orientation and heat treatment on the anisotropic tensile properties of AlSi10Mg fabricated by selective laser melting, J. Alloys Compd. 895 (2022). https://doi.org/10.1016/j.jallcom.2021.162665

[10] G. Tarakçı, H.M. Khan, M.S. Yılmaz and G. Özer, Effect of building orientations and heat treatments on AlSi10Mg alloy fabricated by selective laser melting: Microstructure evolution, mechanical properties, fracture mechanism and corrosion behavior, Rapid Prototyp. J. 28(8) (2022) 1609-1621. https://doi.org/10.1108/RPJ-11-2021-0325

[11] D. Yue, D. Li, X. Zhang, B. Chen, R. Qin and Z. Wang, Tensile behavior of AlSi10Mg overhanging structures fabricated by laser powder bed fusion: Effects of support structures and build orientation, Mater. Sci. Eng. A. 880 (2023) 145375. https://doi.org/10.1016/j.msea.2023.145375

[12] M. Aktürk, M. Boy, M.K. Gupta, S. Waqar, G.M. Krolczyk and M.E. Korkmaz, Numerical and experimental investigations of built orientation dependent Johnson–Cook model for selective

laser melting manufactured AlSi10Mg, JMR&T. 15 (2021) 6244-6259. https://doi.org/10.1016/j.jmrt.2021.11.062

[13] S. Greco, K. Gutzeit, H. Hotz, B. Kirsch and J.C. Aurich, Selective laser melting (SLM) of AISI 316L—impact of laser power, layer thickness, and hatch spacing on roughness, density, and microhardness at constant input energy density, Int. J. Adv. Manuf. Technol. 108(5-6) (2020) 1551-1562. https://doi.org/10.1007/s00170-020-05510-8

[14] R.M. Gouveia, F.J.G. Silva, E. Atzeni, D. Sormaz, J.L. Alves and A.B. Pereira, Effect of Scan Strategies and Use of Support Structures on Surface Quality and Hardness of L-PBF AlSi10Mg Parts, Materials (Basel). 13(10) (2020). https://doi.org/10.3390/ma13102248

[15] H. Jia, H. Sun, H. Wang, Y. Wu and H. Wang, Scanning strategy in selective laser melting (SLM): a review, Int. J. Adv. Manuf. Technol. 113(9-10) (2021) 2413-2435. https://doi.org/10.1007/s00170-021-06810-3

[16] Z. Dong, X. Zhang, W. Shi, H. Zhou, H. Lei and J. Liang, Study of Size Effect on Microstructure and Mechanical Properties of AlSi10Mg Samples Made by Selective Laser Melting, Materials (Basel). 11(12) (2018). https://doi.org/10.3390/ma11122463

[17] N. Takata, H. Kodaira, A. Suzuki and M. Kobashi, Size dependence of microstructure of AlSi10Mg alloy fabricated by selective laser melting, Mater. Charact. 143 (2018) 18-26. https://doi.org/10.1016/j.matchar.2017.11.052

[18] A.M. Roach, B.C. White, A. Garland, B.H. Jared, J.D. Carroll and B.L. Boyce, Size-dependent stochastic tensile properties in additively manufactured 316L stainless steel, Addit. Manuf. 32 (2020). https://doi.org/10.1016/j.addma.2020.101090

[19] D. Barba, C. Alabort, Y.T. Tang, M.J. Viscasillas, R.C. Reed and E. Alabort, On the size and orientation effect in additive manufactured Ti-6Al-4V, Mater. Des. 186 (2020). https://doi.org/10.1016/j.matdes.2019.108235

[20] Information on https://www.tekna.com/

[21] Information on https://www.iso.org/standard/78322.html

[22] Information on https://www.slm-solutions.com

[23] T. Maconachie, M. Leary, J. Zhang, A. Medvedev, A. Sarker, D. Ruan, G. Lu, O. Faruque and M. Brandt, Effect of build orientation on the quasi-static and dynamic response of SLM AlSi10Mg, Mater. Sci. Eng. A. 788 (2020). https://doi.org/10.1016/j.msea.2020.139445

[24] D. Vysochinskiy and N. Akhtar, On the Influence of Cross-Section Size on Measured Strength of SLM-Produced AlSi10Mg-Alloy, KEM. 926 (2022) 132-140. https://doi.org/10.4028/p-g078sc